Crystal Structure and Thermal Properties of Racemic $SrC_4H_4O_6 \cdot 4H_2O$ Single Crystals

T. Fukami[1*], S. Hiyajyo[1], S. Tahara[1] and C. Yasuda[1]

[1]*Department of Physics and Earth Sciences, Faculty of Science, University of the Ryukyus, Okinawa 903-0213, Japan.*

Authors' contributions

This work was carried out in collaboration between all authors. Author TF performed measurements, managed the literature searches and wrote the first draft of the manuscript. Authors SH, ST and CY revised the manuscript and participated in group discussions. All authors have read and approved the final manuscript.

Article Information

Original Research Article

ABSTRACT

Single crystals of racemic strontium tartrate tetrahydrate, $SrC_4H_4O_6 \cdot 4H_2O$, were grown at 308 K by a gel method using silica gel as the medium of growth. Differential scanning calorimetry, thermogravimetric-differential thermal analysis, and X-ray diffraction measurements were performed on the single crystals. The space group symmetry (triclinic $P\bar{1}$) and structural parameters were determined at room temperature. Weight losses due to thermal decomposition were found to occur in the temperature range of 370–1170 K, likely due to the evaporation of bound water molecules and the evolution of H_2CO, $(1/2)O_2$, and $2CO$ gases. The chalky white substance remaining in the vessel after decomposition was strontium oxide SrO. The crystal structure and thermal properties obtained were compared with those of racemic $CaC_4H_4O_6 \cdot 4H_2O$ reported previously.
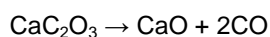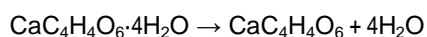
Keywords: Racemic $SrC_4H_4O_6 \cdot 4H_2O$; crystal structure; thermal decomposition; DSC; TG-DTA; X-ray diffraction.

_____

Corresponding author: E-mail: fukami@sci.u-ryukyu.ac.jp;

1. INTRODUCTION

Many tartrate compounds are formed by the reaction of tartaric acid (chemical formula: $C_4H_6O_6$; systematic name: 2,3-dihydroxybutanedioic acid) with compounds containing positive ions (two monovalent cations or one divalent cation) [1-6]. Tartaric acid has two chiral carbon atoms in its structure, which provides the possibility for four possible different forms of chiral, racemic, and achiral isomers: L(+)-tartaric, D(–)-tartaric, racemic (DL-) tartaric, and meso-tartaric acid [6-8]. Some of these compounds are of interest due to their physical properties, particularly their excellent dielectric, ferroelectric, piezoelectric, and nonlinear optical properties [1,9-11]. Moreover, they are used in numerous industrial applications, for example, as transducers and in linear and non-linear mechanical devices [1,4,11]. More than 150 years ago, Louis Pasteur first separated the two enantiomers of sodium ammonium tartrate ($NaNH_4C_4H_4O_6$) by utilizing the asymmetric habit of their crystals [12,13]. In addition, he observed the change in optical rotation induced by the different structures of each enantiomer in solution. The discovery of enantiomers has played an important role in advancing the scientific understanding of molecular chirality.

Using DL-tartaric acid as a crystallization reagent instead of L(+)-tartaric acid, DL-tartaric compounds have been synthesized with a divalent cation [2,14]. We have grown single crystals of racemic (DL-) calcium tartrate tetrahydrate, $CaC_4H_4O_6 \cdot 4H_2O$, by the gel method and have determined the crystal structure at room temperature with space group $P\bar{1}$ [14]. Moreover, it was revealed that the phase transition driven by intramolecular proton transfer between three possible sites occurs around 310 K, and the chemical reactions that take place during thermal decomposition of DL-$CaC_4H_4O_6 \cdot 4H_2O$ are as follows.

$$CaC_4H_4O_6 \cdot 4H_2O \rightarrow CaC_4H_4O_6 + 4H_2O$$

$$CaC_4H_4O_6 \rightarrow CaC_2O_4 + 2H_2CO$$

$$CaC_2O_4 \rightarrow CaC_2O_3 + (1/2)O_2$$

$$CaC_2O_3 \rightarrow CaO + 2CO$$

However, investigations on the crystal growth and physical properties of DL-tartaric compounds other than those of DL-$CaC_4H_4O_6 \cdot 4H_2O$ have not been carried out yet.

In this paper, we describe the synthesis of single crystals of racemic strontium tartrate tetrahydrate, $SrC_4H_4O_6 \cdot 4H_2O$, using the gel method and determine their crystal structure at room temperature using X-ray diffraction. Moreover, the thermal properties of the DL-strontium salt are studied by means of differential scanning calorimetry (DSC) and thermogravimetric-differential thermal analysis (TG-DTA).

2. EXPERIMENTAL

2.1 Crystal Growth

Single crystals of DL-$SrC_4H_4O_6 \cdot 4H_2O$ were grown in silica gel medium at 308 K using the single test tube diffusion method. The gels were prepared in test tubes (length of 200 mm, and diameter of 30 mm) using aqueous solutions of Na_2SiO_3 (20 ml of 1 M), DL-$C_4H_6O_6$ (25 ml of 1 M), and CH_3COOH (25 ml of 1 M), and aged for six days. A solution of $SrCl_2 \cdot 6H_2O$ (40 ml of 0.25 M) was then gently poured on top of the gel. Many small transparent crystals, which are similar to the shapes of DL-$CaC_4H_4O_6 \cdot 4H_2O$ (as seen in Fig. 1 of reference [14]), were grown at the gel matrix-solution interface, and the crystals used (size about $3 \times 1 \times [5 \times 10^{-1}]$ mm) were harvested after about two months.

2.2 Structure Determination

The X-ray diffraction measurements were carried out using a Rigaku Saturn CCD X-ray diffractometer with graphite-monochromated Mo K_α radiation (λ = 0.71073 Å). The diffraction data were collected at 299 K using an ω scan mode with a crystal-to-detector distance of 40 mm, and processed using the CrystalClear software package. The intensity data were corrected for Lorentz polarization and absorption effects. The structure was solved by direct methods using the SIR2011 program and refined on F^2 by full-matrix least-squares methods using the SHELXL-2013 program in the WinGX package [15-17].

2.3 Thermal Measurements

DSC and TG-DTA measurements were carried out in the temperature ranges of 100–490 K and 300–1470 K, respectively, using DSC7020 and TG-DTA7300 systems from Seiko Instruments Inc. Aluminium (for DSC) and platinum (for TG-DTA) open pans with no pan cover were used as measuring vessels and reference pans. Fine powder samples, prepared by grinding single crystals, were used for the measurements. The sample amount varied between 4.09 and 7.46

mg, and the heating rates were 5 or 10 K min^{-1} under a dry nitrogen gas flow.

3. RESULTS AND DISCUSSION

3.1 Crystal Structure

The crystal structure of DL-SrC$_4$H$_4$O$_6$·4H$_2$O was determined at room temperature by the single-crystal X-ray diffraction method. The lattice parameters calculated from all observed reflections indicated that the crystal belongs to triclinic system. The atomic coordinates and thermal parameters for DL-SrC$_4$H$_4$O$_6$·4H$_2$O, including the positions of all hydrogen atoms, were determined with the space group symmetry of triclinic $P\bar{1}$. A final R-factor of 2.80% was calculated for 4354 unique reflections. The relevant crystal data, and a summary of the intensity data collection and structure refinement parameters are given in Table 1. Fig. 1 shows a projected view of the DL-SrC$_4$H$_4$O$_6$·4H$_2$O crystal structure along the *a*-axis. The positional parameters in fractions of the unit cell, and the thermal parameters are listed in Table 2. Selected bond lengths (in Å) and angles (in degrees) are given in Table 3. The hydrogen-bond geometry (in Å and degrees) is presented in Table 4.

The observed lattice parameters and structure are very similar to those of DL-CaC$_4$H$_4$O$_6$·4H$_2$O previously reported, except for small differences in the lattice constants along the *a*- and *b*-axes [14]. The determined structure consists of SrO$_8$ dodecahedra, C$_4$H$_4$O$_6$ and four independent H$_2$O molecules, and O–H⋯O and C–H⋯O hydrogen bonds, similar to the DL-calcium salt. Each Sr atom in the unit cell is surrounded by eight O atoms in the C$_4$H$_4$O$_6$ and H$_2$O molecules at distances from 2.540(1) to 2.639(1) Å, forming the SrO$_8$ dodecahedron (Table 3). The average Sr–O distance is 2.581 Å. The structure of the DL-calcium salt also consists of CaO$_8$ dodecahedra with an average Ca–O distance of 2.450 Å [14]. Thus, the volume of the SrO$_8$ dodecahedron is larger than that of the CaO$_8$ one due to the difference in ionic radii of Sr^{2+} and Ca^{2+} ions.
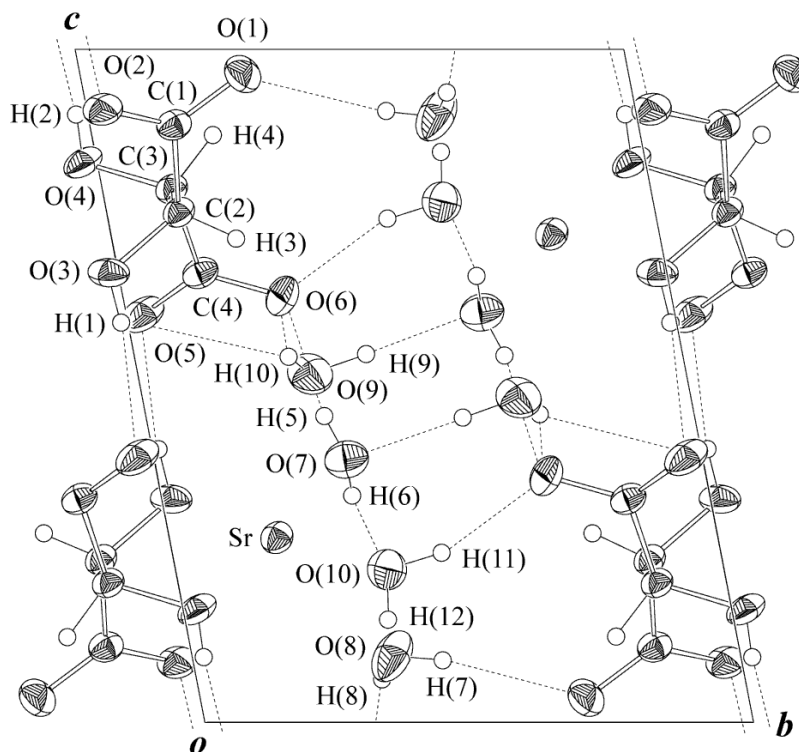
Fig. 1. Projection of the crystal structure of DL-SrC$_4$H$_4$O$_6$·4H$_2$O along the *a*-axis at room temperature with 60% probability-displacement thermal ellipsoids
The solid and dashed short lines show O–H⋯O hydrogen bonds, as described in Table 4

Table 1. Crystal data, intensity collection and structure refinement for DL- SrC$_4$H$_4$O$_6$·4H$_2$O

Compound, M_r	SrO$_{10}$C$_4$H$_{12}$, 307.75
Crystal shape, color	Prism, colorless
Measurement temperature	299 K
Crystal system, space group	Triclinic, $P\bar{1}$
Lattice constants	a = 6.4008(4) Å, b = 8.4251(4) Å, c = 10.4856(5) Å
	α = 95.227(1)$^\circ$, β = 106.386(2)$^\circ$, γ = 107.056(1)$^\circ$
V, Z	509.24(5) Å^3, 2
D(cal.), μ(Mo K_α), F(000)	2.007 Mg m^{-3}, 5.333 mm^{-1}, 308
Crystal size	0.20×0.25×0.30 mm
θ range for data collection	2.06–38.05°
Index ranges	-10 $\le h \le$ 11, -14 $\le k \le$ 14, -17 $\le l \le$ 17
Reflections collected, unique	14779, 5242 [R(int) = 0.0375]
Completeness to θ_{max}	94.3 %
Absorption correction type	Numerical
Transmission factor T_{min}–T_{max}	0.2859–0.4344
Date, parameter	4354 [$I > 2\sigma(I)$], 185
Final R indices	R_1 = 0.0280, wR_2 = 0.0488
R indices (all data)	R_1 = 0.0400, wR_2 = 0.0527
Weighting scheme	w = 1/[$\sigma^2(F_o^2)$+(0.0170P)^2], P = (F_o^2+2F_c^2)/3
Goodness-of-fit on F^2	0.980
Extinction coefficient	0.023(1)
Largest diff. peak and hole	0.503 and -0.741 e Å^{-3}

Table 2. Atomic coordinates and thermal parameters (×10^4 Å^2) at room temperature for DL-SrC$_4$H$_4$O$_6$·4H$_2$O with standard deviations in brackets. The anisotropic thermal parameters are defined as exp[-2π^2($U_{11}a^{*2}h^2$ + $U_{22}b^{*2}k^2$ + $U_{33}c^{*2}l^2$ + $2U_{23}b^*c^*kl$ + $2U_{13}a^*c^*hl$ + $2U_{12}a^*b^*hk$)]. The isotropic thermal parameters (Å^2) for H atoms are listed under U_{11}

Atom	x	y	z	U_{11}	U_{22}	U_{33}	U_{23}	U_{13}	U_{12}
Sr	0.33982(2)	0.19619(2)	0.27454(2)	163.6(6)	206.7(6)	186.5(6)	46.9(4)	33.9(4)	55.0(4)
C(1)	0.6147(2)	0.1537(2)	0.8878(1)	144(5)	235(6)	165(5)	43(4)	29(4)	33(4)
C(2)	0.4165(2)	0.1319(2)	0.7580(1)	164(5)	197(5)	162(5)	52(4)	30(4)	62(4)
C(3)	0.1962(2)	0.1270(2)	0.7927(1)	170(5)	202(5)	154(5)	48(4)	24(4)	63(4)
C(4)	0.0219(2)	0.1497(2)	0.6677(1)	183(6)	253(6)	177(5)	64(4)	48(4)	107(5)
O(1)	0.6983(2)	0.2966(1)	0.9634(1)	251(5)	229(5)	255(5)	-7(4)	-7(4)	34(4)
O(2)	0.6802(2)	0.0295(1)	0.91071(9)	281(5)	298(5)	183(4)	45(4)	-4(4)	153(4)
O(3)	0.3813(2)	-0.0171(1)	0.66821(9)	268(5)	316(5)	144(4)	11(4)	4(3)	156(4)
O(4)	0.0969(2)	-0.0255(1)	0.8318(1)	182(4)	303(5)	175(4)	110(4)	7(3)	28(4)
O(5)	-0.1604(2)	0.0297(1)	0.6061(1)	194(5)	385(6)	238(5)	139(4)	-15(4)	26(4)
O(6)	0.0778(2)	0.2911(1)	0.6336(1)	384(6)	232(5)	288(5)	106(4)	51(4)	130(4)
O(7)	0.1258(2)	0.3508(2)	0.3908(1)	275(6)	361(6)	254(5)	61(5)	65(4)	124(5)
O(8)	0.1794(2)	0.3646(2)	0.0982(1)	273(6)	369(7)	467(7)	217(6)	18(5)	84(5)
O(9)	0.6112(2)	0.3142(2)	0.5175(1)	293(6)	365(6)	303(5)	13(5)	-23(4)	138(5)
O(10)	0.6977(2)	0.3856(2)	0.2272(1)	342(6)	287(6)	292(6)	43(5)	118(5)	12(5)
H(1)	0.327(3)	-0.009(2)	0.595(2)	0.050(6)					
H(2)	0.151(4)	-0.021(3)	0.903(2)	0.049(6)					
H(3)	0.460(3)	0.227(2)	0.719(2)	0.020(4)					
H(4)	0.236(3)	0.221(2)	0.872(2)	0.026(4)					
H(5)	0.106(3)	0.324(3)	0.455(2)	0.043(6)					
H(6)	0.000(4)	0.349(3)	0.338(2)	0.057(7)					
H(7)	0.234(4)	0.453(3)	0.093(2)	0.056(7)					
H(8)	0.041(4)	0.337(3)	0.062(2)	0.060(7)					
H(9)	0.692(4)	0.418(3)	0.543(2)	0.053(6)					
H(10)	0.710(4)	0.279(3)	0.545(2)	0.072(8)					
H(11)	0.752(4)	0.488(3)	0.252(2)	0.058(7)					
H(12)	0.695(3)	0.369(2)	0.154(2)	0.038(5)					

Table 3. Selected interatomic distances (in Å) and angles (in degrees) for DL-SrC$_4$H$_4$O$_6$·4H$_2$O

|			
Sr–O(2)[(1)]	2.540(1)	Sr–O(3)[(1)]	2.639(1)
Sr–O(4)[(2)]	2.592(1)	Sr–O(5)[(2)]	2.544(1)
Sr–O(7)	2.600(1)	Sr–O(8)	2.597(1)
Sr–O(9)	2.554(1)	Sr–O(10)	2.585(1)
Sr–C(1)[(1)]	3.397(1)	Sr–C(4)[(2)]	3.373(1)
O(1) –C(1)	1.255(2)	O(2)–C(1)	1.255(2)
O(3)–C(2)	1.418(2)	O(4)–C(3)	1.410(2)
O(5)–C(4)	1.251(2)	O(6)–C(4)	1.255(2)
C(1)–C(2)	1.529(2)	C(2)–C(3)	1.543(2)
C(3)–C(4)	1.532(2)		
Sr[(1)]–O(2)–C(1)	123.48(8)	Sr[(1)]–O(3)–C(2)	121.13(7)
Sr[(2)]–O(4)–C(3)	121.20(7)	Sr[(2)]–O(5)–C(4)	121.63(8)
Sr[(1)]–C(1)–O(1)	152.86(9)	Sr[(1)]–C(1)–O(2)	38.58(6)
Sr[(1)]–C(1)–C(2)	84.32(7)	Sr[(2)]–C(4)–O(5)	39.96(6)
Sr[(2)]–C(4)–O(6)	155.69(9)	Sr[(2)]–C(4)–C(3)	83.15(7)
O(1)–C(1)–O(2)	125.3(1)	O(1)–C(1)–C(2)	116.3(1)
O(2)–C(1)–C(2)	118.4(1)	O(3)–C(2)–C(1)	109.5(1)
O(3)–C(2)–C(3)	111.7(1)	O(4)–C(3)–C(2)	112.5(1)
O(4)–C(3)–C(4)	109.6(1)	O(5)–C(4)–O(6)	124.6(1)
O(5)–C(4)–C(3)	119.6(1)	O(6)–C(4)–C(3)	115.8(1)
C(1)–C(2)–C(3)	109.8(1)	C(2)–C(3)–C(4)	108.2(1)

(Symmetry codes: (1) -x+1,-y,-z+1; (2) -x,-y,-z+1)

The lengths of all six O–C bonds in the C$_4$H$_4$O$_6$ molecule are in the range of 1.251(2)–1.418(2) Å, as listed in Table 3. The variation in O–C distances is probably related to differences in bond type, matching typical lengths of single and double O–C bonds in organic molecules (around 1.43 and 1.22 Å, respectively). Thus, the O(3)–C(2) and O(4)–C(3) bonds on hydroxyl group have single-bond character, and the remaining four bonds have double-bond character. Moreover, the lengths of three C–C bonds are in the range of 1.529(2)–1.543(2) Å. Because typical C–C single bonds in organic molecules are around 1.54 Å, these three bonds have single-bond character. These bond lengths of the O–C and C–C bonds are very close to those reported for the DL-calcium salt [14]. The angle between the two least-squares planes of atoms, O(1)O(2)O(3)C(1)C(2) and O(4)O(5)O(6)C(3)C(4), in the C$_4$H$_4$O$_6$ molecule was calculated to be 42.52(5)°, compared to 44.76(3)° in the DL-calcium salt. Thus, it can be concluded that the characteristic features of the C$_4$H$_4$O$_6$ molecule in the DL-SrC$_4$H$_4$O$_6$·4H$_2$O crystal are very similar to those in the DL-CaC$_4$H$_4$O$_6$·4H$_2$O crystal [14].

It can be seen in Fig. 1 and Table 4 that O–H···O and C–H···O hydrogen bonds are formed between adjacent molecules (C$_4$H$_4$O$_6$ or H$_2$O) in the crystal structure. The bond lengths of the O–H···O bonds are in the range of 2.683(1)–3.231(2) Å, and of the C–H···O bonds are 3.410(2) and 3.665(2) Å. The lengths of the C–H···O bonds are longer than those of the O–H···O bonds. Thus, the bonding strength of C–H···O is weaker than that of O–H···O since the magnitude of strength is mainly reflected in the bond length. There is a hydrogen-bonding network along the *c*-axis, connected by two types of O–H···O hydrogen bonds (O(3)–H(1)···O(5) and O(4)–H(2)···O(2)) between adjacent C$_4$H$_4$O$_6$ molecules, as shown in Fig. 1. Moreover, four H$_2$O molecules in the structure are located interstitially between two neighboring C$_4$H$_4$O$_6$ molecules, and form nine O–H···O hydrogen bonds with C$_4$H$_4$O$_6$ or other H$_2$O molecules. There is also a hydrogen-bonding network in the [0$\bar{1}$1] direction, consisting of C$_4$H$_4$O$_6$ and H$_2$O molecules linked by the nine O–H···O bonds, as shown in Fig. 1. The structures formed by these hydrogen-bonding networks are very similar to those in the DL-calcium salt [14].

3.2 Thermal Analysis

Fig. 2 shows the DSC curve of the DL-SrC$_4$H$_4$O$_6$·4H$_2$O crystal upon heating from 100 to 490 K. The sample weight (powder) used for the measurement was 7.45 mg, and the heating rate was 5 K min^{-1} under a nitrogen gas flow of 40 ml min^{-1}. Three large endothermic peaks are clearly seen in the DSC curve at 376.3, 408.8, and 431.4 K. The total enthalpy (*ΔH*) for the three peaks was determined to be 172.3 kJ mol^{-1}. Moreover, the *ΔH* values of 23.7, 62.6, and 86.1 kJ mol^{-1} corresponding to the three peaks were
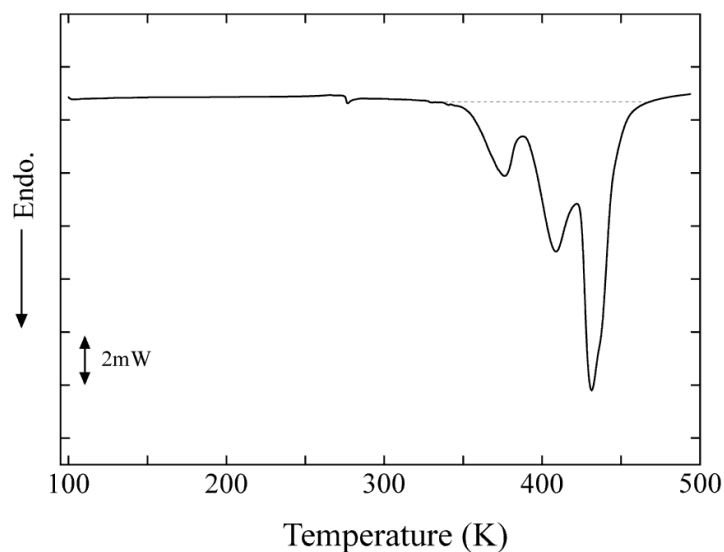
Fig. 2. DSC curve for DL-SrC$_4$H$_4$O$_6$·4H$_2$O crystal on heating
The sample weight (powder) was 7.45 mg, and the heating rate was 5 K min^{-1} under a dry N$_2$ flux of 40 ml min^{-1}

Table 4. Hydrogen bond distances (in Å) and angles (in degrees)

D–H···A	D–H	H···A	D···A	<D–H···A
O(3)–H(1)···O(5)[1]	0.76(2)	2.05(2)	2.800(1)	171(2)
O(4)–H(2)···O(2)[2]	0.72(2)	1.97(2)	2.683(1)	172(2)
C(2)–H(3)···O(9)	0.94(2)	2.63(2)	3.410(2)	140(1)
C(3)–H(4)···O(8)[3]	1.01(2)	2.73(2)	3.665(2)	154(1)
O(7)–H(5)···O(6)	0.76(2)	1.97(2)	2.723(2)	172(2)
O(7)–H(6)···O(10)[4]	0.83(2)	2.08(2)	2.907(2)	170(2)
O(8)–H(7)···O(1)[5]	0.74(2)	2.19(2)	2.914(2)	164(2)
O(8)–H(8)···O(1)[6]	0.81(2)	2.05(2)	2.858(2)	172(2)
O(9)–H(9)···O(7)[5]	0.85(2)	1.90(2)	2.744(2)	177(2)
O(9)–H(10)···O(5)[7]	0.77(3)	2.55(3)	3.231(2)	149(2)
O(9)–H(10)···O(6)[7]	0.77(3)	2.24(2)	2.962(2)	156(2)
O(10)–H(11)···O(6)[5]	0.81(2)	1.94(2)	2.722(2)	161(2)
O(10)–H(12)···O(1)[8]	0.76(2)	2.05(2)	2.801(2)	172(2)

(Symmetry codes: (1) -x,-y,-z+1; (2) -x+1,-y,-z+2; (3) x,y,z+1; (4) x-1,y,z; (5) -x+1,-y+1,-z+1; (6) x-1,y,z-1; (7) x+1,y,z; (8) x,y,z-1)

obtained from the peak separation procedure in the DSC curve, and entropies (*ΔS*) of 7.58*R*, 18.4*R*, and 24.0*R* were calculated using the *ΔH* values, where *R* is the gas constant (8.314 JK^{-1} mol^{-1}). Table 5 shows the peak temperatures, enthalpies, and entropies determined from the DSC curve. The three-peak structure observed differs from the DSC curve of the DL-calcium salt which showed only one endothermic peak at 387.8 K with an enthalpy change of 136.6 kJ mol^{-1} [14]. The enthalpy change (*ΔH*=172.3 kJ mol^{-1}) around 410 K in the DL-strontium salt is also larger than that in the DL-calcium salt, which is likely due to slight underestimation of the DSC peak area in the DL-calcium salt caused by decreased uncertainty in the baseline.

Table 5. Peak temperatures, and transformation enthalpies *ΔH* and entropies *ΔS* for DL-SrC$_4$H$_4$O$_6$·4H$_2$O obtained from DSC, DTA and DTG curves

DSC	Peak temp. (K)	376.3	408.8	431.4					
	ΔH (kJ mol^{-1})	23.7	62.6	86.1					
	ΔS/R	7.58	18.4	24.0					
DTA	Peak temp. (K)	377.9	405.1	437.4	565.2	741.0	761.7	1086.5	1164.9
DTG	Peak temp. (K)	375.8	403.8	436.3	563.5	737.5	761.6	1082.4	1159.3

(Gas constant R = 8.314 JK^{-1}mol^{-1})

In general, it is believed that a distinct peak in a DSC curve can be attributed to the change in exchange energy at phase transition. Therefore, the results indicate that the transformations in DL-SrC$_4$H$_4$O$_6$·4H$_2$O take place at around 376, 409, and 431 K, and that there is no transition in the temperature range of 100–376 K. The transition temperature of 376.3 K is very close to the boiling point of water (373 K), so we attribute the three peaks in the temperature range of 376–431 K to the evaporation of bound water molecules from the sample. This is confirmed by the weight loss observed around 410 K in the TG curve (Table 6). Since there are eight water molecules in the unit cell, the ΔH value per water molecule is estimated to be 21.5 kJ mol^{-1}, adding up to the total enthalpy 172.3 kJ mol^{-1} observed. We assume that the peaks in the range of 376–431 K are produced by the evaporation losses of one, three, and four water molecules. Then, the ΔH value corresponding to each peak can be calculated to be 21.5, 64.5, and 86.0 kJ mol^{-1} (1×21.5, 3×21.5, and 4×21.5 kJ mol^{-1}, respectively). These values are very close to those obtained from the peak separation procedure in the curve (Table 5). Thus, it can be concluded that the weight losses of one, three, and four bound water molecules due to evaporation are driven by increasing temperature in the range of 376–431 K. Moreover, the difference in evaporation temperature of the eight water molecules is probably caused by the difference in hydrogen-bonding strengths connecting the water molecules. The hydrogen-bonding strength is mainly influenced by O⋯O distance of the bond. The bond lengths of the O–H⋯O hydrogen bonds in the DL-strontium and DL-calcium salts are in the ranges of 2.722(2)–3.231(2) Å (shown in Table 4) and 2.731(1)–3.205(1) Å, respectively [14]. The maximum difference among the lengths in the DL-calcium salt is smaller than that in the DL-strontium salt. We consider that the evaporation of all the water molecules takes place at only one temperature when the bond lengths have almost the same value and, therefore, similar strengths. We can conclude that the difference in the DSC peak structure between the DL-strontium and DL-calcium salts is probably related to the differences in hydrogen-bond lengths.

A very small endothermic peak at 276.8 K is also seen on the DSC curve in Fig. 2, which is very close to 273 K. We observed a complete disappearance of the small peak in the curve of the sample dried at room temperature, as well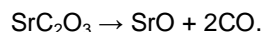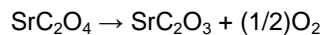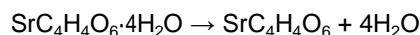 as an increase of peak intensity at 376.3 K and a decrease of peak intensity at 431.4 K. In general, there are many defects in the crystal structure, such as pores and cracks, and the aqueous solution used for crystal growth can infiltrate these defects. The very small peak at 276.8 K may be produced by the state change of the infiltrated solution from a solid (frozen state) to liquid in the defects of the DL-SrC$_4$H$_4$O$_6$·4H$_2$O crystal upon heating.

We have recently reported the results from DSC and X-ray measurements of DL-CaC$_4$H$_4$O$_6$·4H$_2$O [14]. The value of ΔS for the small endothermic peak around 310 K observed in the DSC curve was determined to be 1.05R, which is very close to R ln 3 (1.10R). The position of the H(1) atom bonded to the O(3) atom was determined by X-ray structural analysis, and moreover, two anomalous residual electron density peaks in the vicinity of the O(2) and O(3) atoms were found in the difference Fourier map after the final refinement cycle. The distances between the atoms and detected peak positions were all around 1.0 Å, the O(3)–H(1) bond was 0.82(2) Å, and the distance between the O(3) atom and one of the peak positions was 1.02 Å. The angle formed at the O(3) atom by the H(1) atom and the peak position was 137°. Furthermore, the distance between the O(2) atom and the other peak position was 0.94 Å, and the distance between the two peaks was 1.13 Å. From these results the number of steady states of the H atom was suggested to vary from one to three possible positions at the phase transition around 310 K. However, no endothermic peak corresponding to the small peak around 310 K is observed in the DSC curve of the DL-strontium salt (Fig. 2). Moreover, residual electron density peaks near those observed in the DL-calcium salt were not found in the difference Fourier map during the refinement procedure.

The two density peaks were nearly located on the line connecting the O and Ca atoms. The angles formed at the peak position by the O and Ca atoms in the O(2)–Ca and O(3)–Ca bonds were 128° and 142°, respectively. The bonds formed between oppositely charged O^{2-} and Ca^{2+} ions in the DL-calcium salt possess both ionic and covalent characteristics. There is localized low electron density around the H atom in the hydrogen bond, which is calculated as a difference Fourier peak in the X-ray refinement procedure. The electrons belonging to the covalent bond between the O^{2-} and Ca^{2+} ions may relate to the electron density around the H atom given its existence probability. The bond

lengths of the O(2)–Sr and O(3)–Sr bonds in the DL-strontium salt are 2.540(1) and 2.639(1) Å, as shown in Table 4, and are longer by about 0.1 Å than those of the O(2)–Ca and O(3)–Ca bonds at 2.4011(7) and 2.5261(7) Å, respectively. The electron density in the bonding orbital located between the O^{2-} and Sr^{2+} ions is smaller than that between the O^{2-} and Ca^{2+} ions because the Sr^{2+} and Ca^{2+} ions have the same magnitude (+2e) of charge. Consequently, the residual electron density peaks on the O(2)–Sr and O(3)–Sr bonds are not observed around the peak positions found in the DL-calcium salt. Then, we consider that no phase transition in the DL-strontium salt is closely related to the difference in length between the O–Sr and O–Ca bonds.

Fig. 3 shows the DTA, TG, and differential TG (DTG) curves of the DL-$SrC_4H_4O_6\cdot4H_2O$ crystal in the temperature range of 300–1470 K. The sample weight (powder) used for the measurement was 7.46 mg, and the heating rate was 10 K min^{-1} under a nitrogen gas flow of 400 ml min^{-1}. The DTA curve exhibits eight endothermic peaks at 377.9, 405.1, 437.4, 565.2, 741.0, 761.7, 1086.5, and 1164.9 K, including small peaks. The peak structure around 410 K in the DTA curve is very similar to that in the DSC curve of Fig. 2. Moreover, eight peaks at 375.8, 403.8, 436.3, 563.5, 737.5, 761.6, 1082.4, and 1159.3 K, including very small peaks, are observed in the DTG curve. These DTG peaks almost correspond to the respective DTA peaks. The DTG curve, which is the first derivative of TG curve, reveals the temperature dependence of the rate of weight loss. Thus, the DTA peaks are associated with the maximum rate of weight loss in the TG curve due to thermal decomposition of the sample. The peak temperatures obtained from the DTA and DTG curves were added to Table 5. The TG curve shows the temperature dependence of the weight loss for the DL-$SrC_4H_4O_6\cdot4H_2O$ crystal. According to the chemical reactions for decomposition of DL-$CaC_4H_4O_6\cdot4H_2O$ as mentioned in the introduction, we assume that the chemical processes involved in the decomposition of DL-$SrC_4H_4O_6\cdot4H_2O$ can be described by the following equations [14]:

$$SrC_4H_4O_6\cdot4H_2O \rightarrow SrC_4H_4O_6 + 4H_2O$$

$$SrC_4H_4O_6 \rightarrow SrC_2O_4 + 2H_2CO$$

$$SrC_2O_4 \rightarrow SrC_2O_3 + (1/2)O_2$$

$$SrC_2O_3 \rightarrow SrO + 2CO.$$

The experimental weight losses obtained from the TG analysis, the theoretical losses based on the chemical reactions above, and the molecular gases eliminated at various temperature ranges are summarized in Table 6. The theoretical loss values calculated for each temperature range match closely with the experimental data. The slight differences between the experimental and theoretical values at each temperature range are probably a result of overlapping temperature ranges corresponding to the decomposition reactions. After heating the sample up to 1470 K, a chalky white substance was found in the open vessel. The white substance is strontium oxide SrO, as suggested by the chemical equations as described above.

The thermal decompositions of the DL-strontium and DL-calcium salts were observed in different temperature ranges of approximately 370–1170 and 390–970 K [14]. The difference in the temperature ranges is caused by the decomposition above 900 K. The peak temperatures and weight loss profiles between 500 and 900 K are very similar in the two salts, and the evolved gases during the thermal decomposition of $C_4H_4O_6$, as described by the second and third equations, are qualitatively and quantitatively the same. The decomposition temperature (1159.3 K) of the DL-strontium salt is higher by about 200 K than for the DL-calcium salt (964.4 K), and the decomposition reaction is shown as the last equation mentioned above. The experimental data suggest that evolution of 2CO gas molecules from the DL-strontium and DL-calcium salts is exactly the same, and the only major difference is in the final decomposition reaction product (SrO or CaO). The difference in the decomposition temperature indicates that the production of SrO requires higher temperatures than for CaO.

Table 6. TG results of thermal decomposition process of DL-$SrC_4H_4O_6\cdot4H_2O$

Temp. range [K]	Weight loss (obs.)[%]	Weight loss (cal.) [%]	Elimination molecules
300-500	23.5	23.4	$4H_2O$
500-680	18.0	19.5	$2H_2CO$
680-900	7.3	5.2	$(1/2)O_2$
900-1300	19.6	18.2	2CO
Total	68.4	66.3	
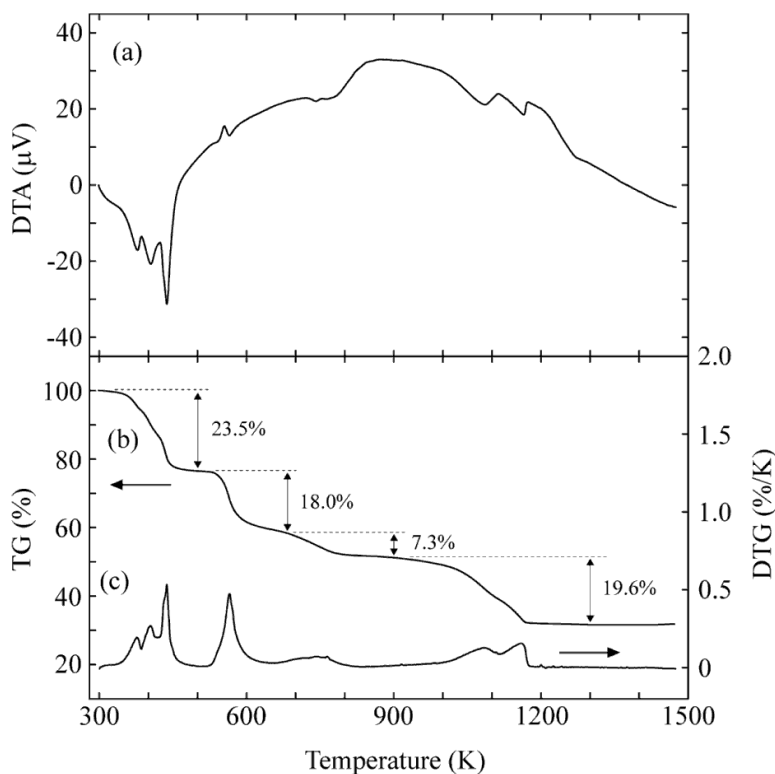
Fig. 3. TG, DTG, and DTA thermograms for DL-SrC$_4$H$_4$O$_6$·4H$_2$O crystal on heating
The sample weight (powder) was 7.46 mg, and the heating rate was 10 Kmin^{-1} under a dry N$_2$ flux of 400 ml min^{-1}

4. SUMMARY

Single crystals of racemic strontium tartrate tetrahydrate, SrC$_4$H$_4$O$_6$·4H$_2$O, were grown in silica gel medium by gel technique at 308 K. The thermal properties and crystal structure of the single crystals were studied by DSC, TG-DTA, and X-ray diffraction. The crystal structure at room temperature, including the positions of the hydrogen atoms, was determined to be triclinic with space group $P\bar{1}$ by means of single-crystal X-ray diffraction, and found to consist of SrO$_8$ dodecahedra, C$_4$H$_4$O$_6$ and four independent H$_2$O molecules, and hydrogen-bonding networks that are connected between adjacent C$_4$H$_4$O$_6$ molecules along the *c*-axis and between C$_4$H$_4$O$_6$ and H$_2$O molecules along the [0$\bar{1}$1] direction. Weight losses during the thermal decomposition of DL-SrC$_4$H$_4$O$_6$·4H$_2$O crystals occur in the temperature range of 370–1170 K. It is suggested that the weight losses are caused by the evaporation of bound water molecules and the evolution of 2H$_2$CO, (1/2)O$_2$, and 2CO gases, and the resulting chalky white substance in the vessel after decomposition is strontium oxide SrO. The crystal structure and thermal properties observed in this study are very similar to those of racemic CaC$_4$H$_4$O$_6$·4H$_2$O previously reported, except for the phase transition around 310 K, the DSC peak structure for water evaporation around 390 K, and the difference in the decomposition temperature range [14].

COMPETING INTERESTS

Authors have declared that no competing interests exist.

REFERENCES

1. Desai CC, Patel AH. Crystal data for ferroelectric RbHC$_4$H$_4$O$_6$ and NH$_4$HC$_4$H$_4$O$_6$ crystals. J Mater Sci Lett. 1988;7(4):371–373.
2. Bail AL, Bazin D, Daudon M, Brochot A, Robbez-Massond V, Maisonneuve V. Racemic calcium tartrate tetrahydrate [form (II)] in rat urinary stones. Acta Crystallogr. 2009;B65(3):350–354.
3. Labutina ML, Marychev MO, Portnov VN, Somov NV, Chuprunov EV. Second-order nonlinear susceptibilities of the crystals of some metal tartrates. Crystallogr Rep. 2011;56(1):72–74.

4. Fukami T, Tahara S, Yasuda C, Nakasone K. Crystal structure and thermal properties of $SrC_4H_4O_6 \cdot 4H_2O$ single crystals. Int Res J Pure Appl Chem. 2016;11(1):23674:1–10.

5. Fukami T, Hiyajyo S, Tahara S, Yasuda C. Thermal properties and crystal structure of $BaC_4H_4O_6$ single crystals. Inter J Chem. 2017;9(1):30–37.

6. Fukami T, Tahara S, Yasuda C, Nakasone K. Structural refinements and thermal properties of L(+)-tartaric, D(–)-tartaric, and monohydrate racemic tartaric acid. Inter J Chem. 2016;8(2):9–21.

7. Bootsma GA, Schoone JC. Crystal structures of mesotartaric acid. Acta Crystallogr. 1967;22(4):522–532.

8. Song QB, Teng MY, Dong Y, Ma CA, Sun J. (2S,3S)-2,3-Dihydroxy-succinic acid monohydrate. Acta Crystallogr. 2006; E62(8):o3378–o3379.

9. Abdel-Kader MM, El-Kabbany F, Taha S, Abosehly AM, Tahoon KK, El-Sharkawy AA. Thermal and electrical properties of ammonium tartrate. J Phys Chem Solids. 1991;52(5):655–658.

10. Torres ME, Peraza J, Yanes AC, López T, Stockel J, López DM, Solans X, Bocanegra E, Silgo GG. Electrical conductivity of doped and undoped calcium tartrate. J Phys Chem Solids. 2002;63(4):695–698.

11. Firdous A, Quasim I, Ahmad MM, Kotru PN. Dielectric and thermal studies on gel grown strontium tartrate pentahydrate crystals. Bull Mater Sci. 2010;33(4):377–382.

12. Pasteur ML. Sur les relations qui peuvent existre la forme cristalline, la composition chimique et Le sens de la polarisation rotatoire. Ann Chim Phys. 1848;24:442–463.

13. Gal J. Citation for chemical breakthrough awards: Choosing pasteur's award-winning publication. Bull Hist Chem. 2013;38(1):7–12.

14. Fukami T, Hiyajyo S, Tahara S, Yasuda C. Thermal properties, crystal structure, and phase transition of racemic $CaC_4H_4O_6 \cdot 4H_2O$ single crystals. Am Chem Sci J. 2016;16(3):28258:1–11.

15. Burla MC, Caliandro R, Camalli M, Carrozzini B, Cascarano GL, Giacovazzo C, Mallamo M, Mazzone A, Polidori G, Spagna R. SIR2011: A new package for crystal structure determination and refinement. J Appl Crystallogr. 2012;45(2): 357–361.

16. Sheldrick GM. Crystal structure refinement with SHELXL. Acta Crystallogr. 2015; C71(1):3–8.

17. Farrugia LJ. WinGX and ORTEP for Windows: An update. J Appl Crystallogr. 2012;45(4):849–854.

_____